Wave kinetics of drift-wave turbulence and zonal flows beyond the ray approximation

Hongxuan Zhu[1,2], Yao Zhou[2], D. E. Ruiz[3], and I. Y. Dodin[1,2].

[1]Princeton University [2]Princeton Plasma Physics Laboratory [3]Sandia National Laboratories

Overview

- We report quasilinear modeling of inhomogeneous drift-wave (DW) turbulence and zonal flows (ZFs) in *phase space with full-wave effects retained.*
- Specifically, by applying the Wigner–Moyal approach to the Hasegawa-Mima equation, we treat DW turbulence as quantumlike plasma, where the ZF velocity acts as a collective field.
- Our results improve the understanding of the zonostrophic instability, tertiary instability, and predator-prey oscillations. Full-wave effects determined by the ZF wavenumber q are found to be critical.

generalized Hasegawa–Mima equation (gHME)

- Can be used to study some aspects of the ITG–ZF interactions.
- Electrostatic fluctuations on the $x-y$ plane. Ions: $\boldsymbol{E}\times\boldsymbol{B}$ and polarization drift. Electrons: adiabatic response $\delta n_e = |e|\delta\varphi/T_e$ except for ZFs.

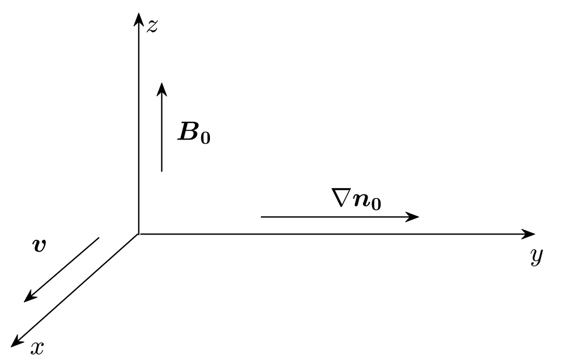

$$\frac{\partial w}{\partial t} + \beta\frac{\partial \varphi}{\partial x} + (\hat{\boldsymbol z}\times\nabla\varphi)\cdot\nabla w = Q \qquad (1)$$

$w \doteq (\nabla^2 - \hat a)\varphi$: generalized vorticity,

$\hat a f \doteq f - \langle f\rangle$, $\quad \langle f\rangle \doteq \frac{1}{L_x}\int_0^{L_x} f\,dx$.

- Conserved quantities ($Q=0$): energy and enstrophy:

$$E \doteq \frac{1}{2}\int d^2x\,[(\nabla\varphi)^2 + (\hat a\varphi)^2], \quad \mathcal{Z} \doteq \frac{1}{2}\int d^2x\, w^2.$$

- φ is normalized by $T_e/|e|$; length unit: ion sound radius ρ_s; time unit: inverse ion gyrofrequency Ω_i^{-1}; β: density gradient.

The role of q in tertiary instability (TI)

- The TI is the instability of a strong prescribed ZF. It is of interest due to its potential role in finite Dimits shift, Ref. [1] has some historical discussions.
- Problem setup: linearizing the gHME on a stationary ZF velocity $U(y)$, assuming the perturbation is $\tilde\varphi = \phi(y)\exp(ik_x x - i\omega t)$. Then,

$$\left(\frac{d^2}{dy^2} - 1 - k_x^2 - \frac{U''-\beta}{U-\omega/k_x}\right)\phi(y) = 0. \qquad (2)$$

- Assume $U = u_0\cos qy$. By following and correcting Ref. [2], the TI growth rate is approximately

$$\gamma_{\mathrm{TI},1} = |k_x u_0|\vartheta H(\vartheta)\sqrt{1-\varrho^{-2}}, \qquad (3)$$

where $\vartheta \doteq 1 - (\bar q^2 + 1 + k_x^2)/q^2$, $\varrho = u_0 q^2/\beta$, and H is the Heaviside step function.

- Two necessary conditions for the TI are: (i) the Rayleigh–Kuo criterion, namely, $U'' = \beta$ is satisfied somewhere (i.e., $q^2 u_0 > \beta$); also, (ii) $q > 1$.
- An alternative approximation of γ_{TI} is mentioned in Ref. [1]:

$$\gamma_{\mathrm{TI},2} = |k_x u_0|[\sqrt{2}(1+\delta)]^{-1}\sqrt{1-\delta^2-(2\delta^2\varrho^2)^{-1}}. \qquad (4)$$

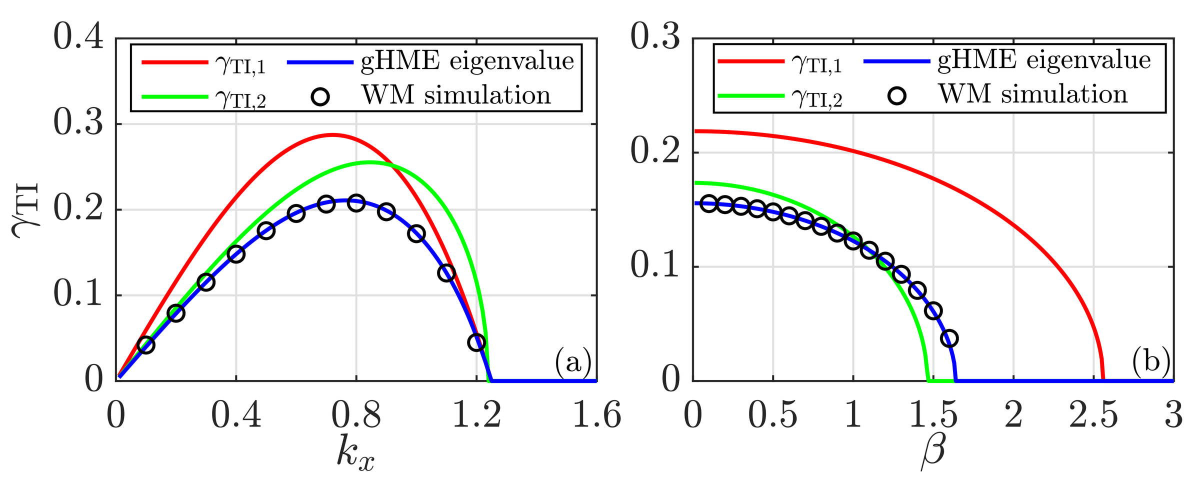

Figure 1: (a) $\gamma_{\mathrm{TI}}(k_x)$ at $\beta = 0.5$ and (b) $\gamma_{\mathrm{TI}}(\beta)$ at $k_x = 0.4$. In both cases, $U(t=0,y) = u_0\cos qy$, $u_0 = 1$, $q = 1.6$, and $\bar q = 0$.

- Qualitatively similar conclusions apply to non-sinusoidal ZFs.

The Wigner function

- The Wigner function is obtained through the Weyl transform:

$$W(\boldsymbol{x},\boldsymbol{p},t) = \int d\boldsymbol{s}\, e^{-i\boldsymbol{p}\cdot\boldsymbol{s}} w(\boldsymbol{x}+\boldsymbol{s}/2)w(\boldsymbol{x}-\boldsymbol{s}/2), \qquad \int dp\, W(x,p,t)/(2\pi) = w^2(x).$$

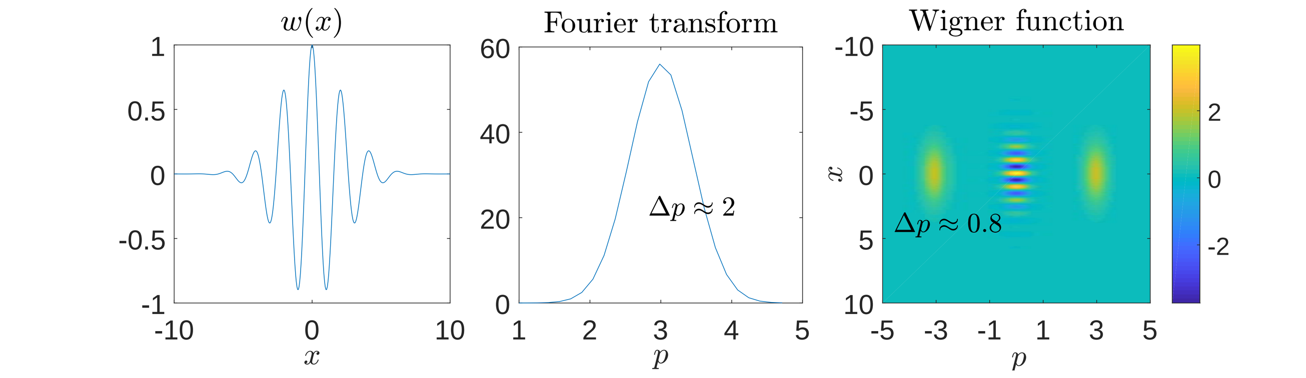

The quasilinear Wigner–Moyal (WM) formulation [3]

- The fluctuation part of the gHME ($Q = 0$, $\boldsymbol{v} \doteq \hat{\boldsymbol z}\times\nabla\varphi$):

$$\partial_t\tilde w + \bar{\boldsymbol v}\cdot\nabla\tilde w + \tilde{\boldsymbol v}\cdot\nabla\bar w + \beta\partial_y\tilde\varphi + f_{\mathrm{NL}} = 0, \quad f_{\mathrm{NL}} \doteq \tilde{\boldsymbol v}\cdot\tilde{\boldsymbol w} - \overline{\tilde{\boldsymbol v}\cdot\tilde{\boldsymbol w}}.$$

Quasilinear approximation: $f_{\mathrm{NL}} \approx 0$. Then (with $U \doteq -\partial_y\bar\varphi$),

$$\partial_t\tilde w + U\partial_x\tilde w + [\beta - (\partial_y^2 U)]\partial_x\tilde\varphi = 0 \quad\Rightarrow\quad i\partial_t\tilde w = \hat{\mathcal H}\tilde w. \qquad (5)$$

Zonal-averaged part of gHME:

$$\partial_t\bar w + \overline{\tilde{\boldsymbol v}\cdot\tilde{\boldsymbol w}} = 0 \quad\Rightarrow\quad \partial_t U = -\partial_y\overline{\tilde v_x\tilde v_y}. \qquad (6)$$

- (Zonal-averaged) WM equations ($W = (y,\boldsymbol p,t)$):

$$\frac{\partial W}{\partial t} = \{\{\mathcal H, W\}\} + [[\Gamma, W]], \quad \frac{\partial U}{\partial t} = \frac{\partial}{\partial y}\int\frac{d^2p}{(2\pi)^2}\frac{p_x}{p_D^2}\star W\star\frac{p_y}{p_D^2}. \qquad (7)$$

where $p_D^2 = 1 + p_x^2 + p_y^2$, $\star \doteq \exp(i\hat{\mathcal L}/2)$, and

$$\mathcal H = -\beta p_x/p_D^2 + p_x U + \frac{1}{2}[[U'', p_x/p_D^2]], \quad \Gamma = \frac{1}{2}\{\{U'', p_x/p_D^2\}\},$$

$$\{\{A,B\}\} = 2A\sin(\hat{\mathcal L}/2)B, \quad [[A,B]] = 2A\cos(\hat{\mathcal L}/2)B.$$

$$\hat{\mathcal L} \doteq \overleftarrow{\partial}_{\boldsymbol x}\cdot\overrightarrow{\partial}_{\boldsymbol p} - \overleftarrow{\partial}_{\boldsymbol p}\cdot\overrightarrow{\partial}_{\boldsymbol x}, \text{ e.g., } A\hat{\mathcal L}B = \{A,B\}.$$

- The WM is equivalent to CE2 [4], but describes physics in phase space.

The improved wave-kinetic equation (iWKE)

- Ray approximation (or GO limit): $q \ll \min(\lambda_{\mathrm{DW}}^{-1}, 1)$, then $\{\{A,B\}\} \approx \{A,B\} = \partial_{\boldsymbol x}A\cdot\partial_{\boldsymbol p}B - \partial_{\boldsymbol p}A\cdot\partial_{\boldsymbol x}B$, $[[A,B]] \approx 2AB$. And

$$\frac{\partial W(y,\boldsymbol p,t)}{\partial t} = \{\mathcal H, W\} + 2\Gamma W, \quad \frac{\partial U(y,t)}{\partial t} = \frac{\partial}{\partial y}\int\frac{d^2p}{(2\pi)^2}\frac{p_x p_y W}{p_D^4}. \qquad (8)$$

"Drifton" Hamiltonian (the terms in red are missed in the traditional WKE):

$$\mathcal H(y,t) = -\beta p_x/p_D^2 + p_x U + p_x U''/p_D^2, \quad \Gamma(y,t) = -p_x p_y U'''/p_D^4. \qquad (9)$$

The role of q in zonostrophic instability (ZI)

- The iWKE fixes the "ultraviolet divergence" issue of the tWKE in modeling ZI [4]. However, even the iWKE differs from WM once $q \sim 1$.

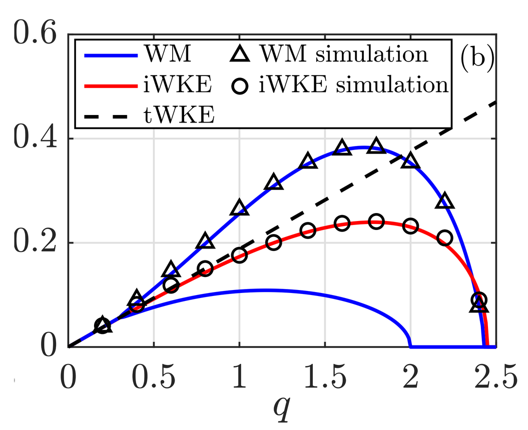

Dispersion relation of ZI from WM:

$$\gamma_{\mathrm{ZI}} = \int\frac{d^2p}{(2\pi)^2}\frac{q p_x^2 p_y}{\gamma_{\mathrm{ZI}} p_{D,+q}^2 p_{D,-q}^2 + 2i\beta q p_x p_y}\times\left[\left(1 - q^2/p_{D,-q}^2\right)\mathcal W_{-q} - \left(1 - q^2/p_{D,+q}^2\right)\mathcal W_{+q}\right]$$

- An example: $\mathcal W(\vec p) = \pi^2\mathcal N\sum_{m_{x,y}=\pm1}\delta(p_x - m_x k_x)\delta(p_y - m_y k_y)$. The parameters are $\beta = 1$, $k_x = 2$, $k_y = 1$, $\mathcal N = 100/2\pi^2$.

The predator–prey (pp) oscillation is observed from collisionless quasilinear WM simulations.

- Numerical simulation of the ZI (Fig. 3) and TI (Fig. 4). In Fig. 3, solid lines are from WM simulations, while dashed lines are from iWKE simulations using GKEYLL [5].
- For ZI, the iWKE always predict that the ZF saturates, while WM simulations show that the ZF bounces back if $q > 1$. For TI, the PP oscillation are almost always seen, since the TI requires $q > 1$.

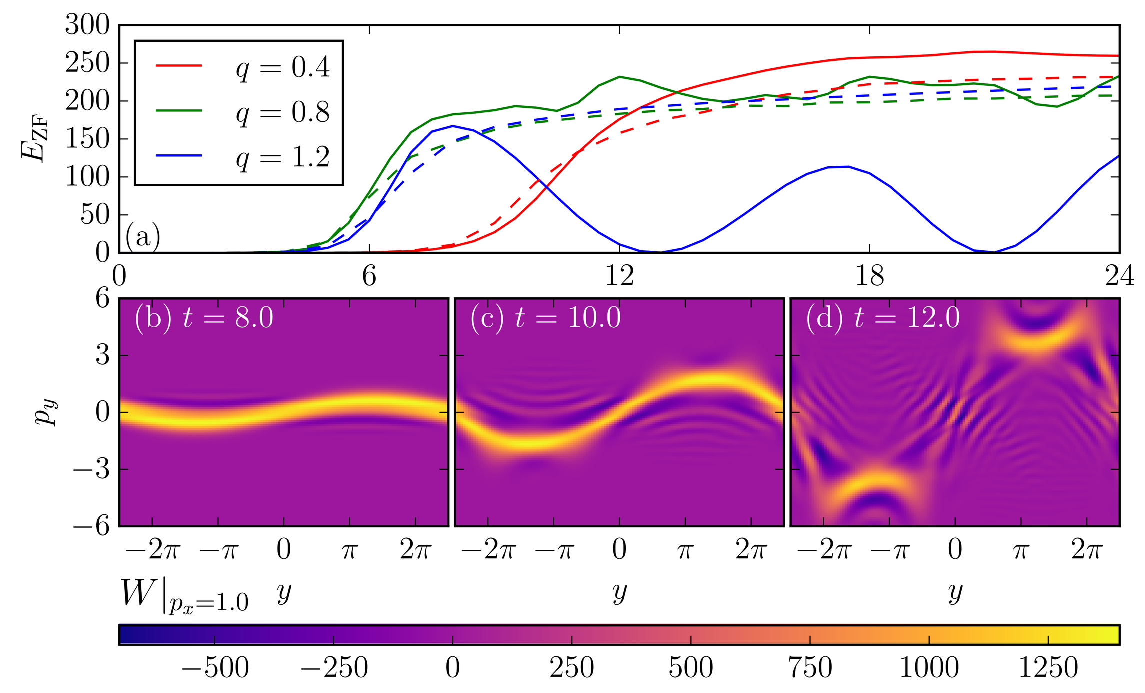

Figure 3: The initial conditions are $\mathcal W(\vec p) = 2\pi\mathcal N\delta(|\vec p| - p_f)/p_f$ and $U = U_q\cos qy$ ($U_q \ll 1$). The parameters are $\mathcal N = 50$, $p_f = 1$, $\beta = 1$.

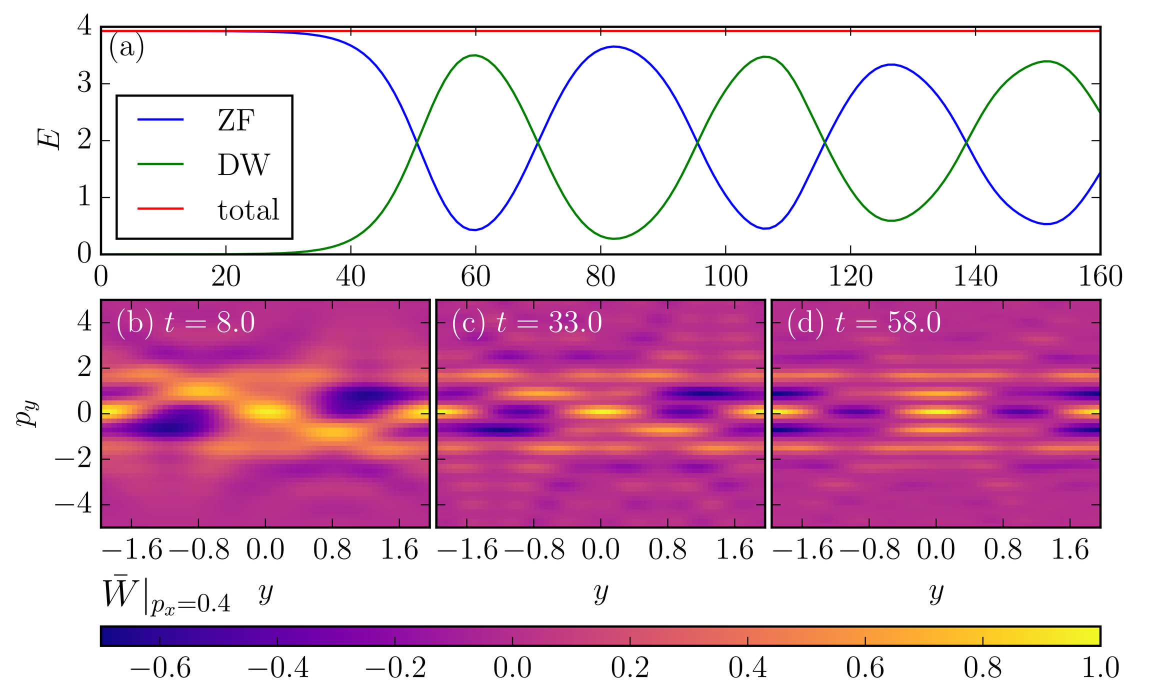

Figure 4: Initially $U = u_0\cos qy$ and $W = W_0\exp(-p_y^2)\delta(p_x \pm k_x)$ ($W_0 \ll 1$). The parameters are $q = 1.6$, $u_0 = 1$, $\beta = 1$, $k_x = 0.4$.

The importance of ZF wavenumber q during the PP oscillation

- iWKE ray trajectories qualitatively elucidate why V_{ZF} increases monotonically.

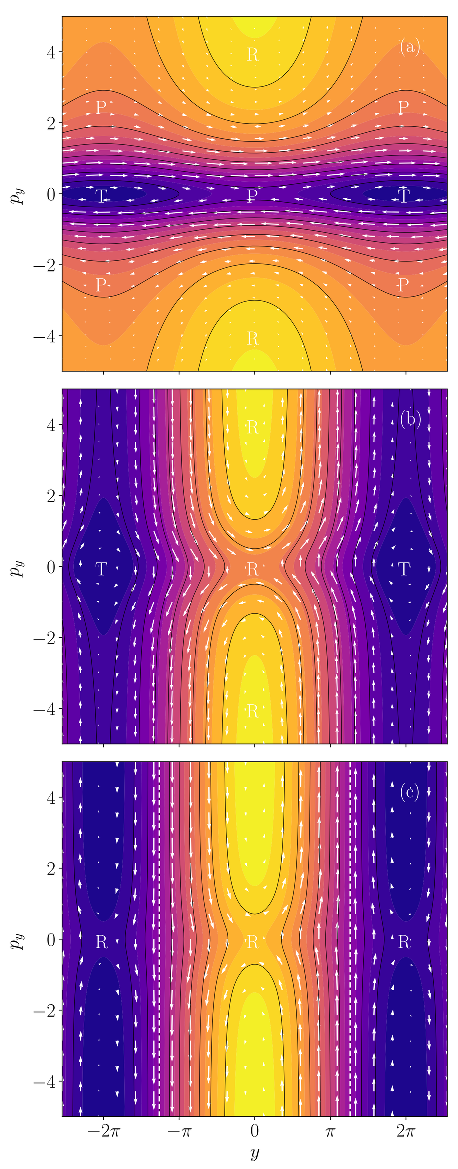

Figure 5: Constant $\mathcal H$ surfaces [Eq. (9)] with $U = u_0\cos qy$. Three different regimes are identified based on u_0.

- A simple PP model from Ref. [6] based on the traditional WKE:

$$\partial_t\mathcal E = \mathcal E\mathcal N - a_1\mathcal E^2 - a_2V^2\mathcal E - a_3V_{\mathrm{ZF}}^2\mathcal E, \quad \partial_t V_{\mathrm{ZF}} = b_1\mathcal E V_{\mathrm{ZF}}/(1 + b_2V^2) - b_3V_{\mathrm{ZF}},$$
$$\partial_t\mathcal N = -c_1\mathcal E\mathcal N - c_2\mathcal N + Q, \quad V = d\mathcal N^2.$$

- $\mathcal E$: DW energy, V_{ZF}: ZF velocity, V: mean flow velocity, and $\mathcal N$: pressure gradient (free energy).
- b_3 is the ZF collisional damping. V_{ZF} increases monotonically if $b_3 = 0$. However, from WM simulations, the PP oscillation is observed *even if* there is no ZF damping, i.e., $b_3 = 0$.
- $q < 1$: The strong coupling of different spectral components results in the advection of DW into large p_y and λ regions. This is related to runaway trajectories and associated with the ZF saturation.
- $q > 1$: The weak coupling results in localized (PP) oscillations in phase space.

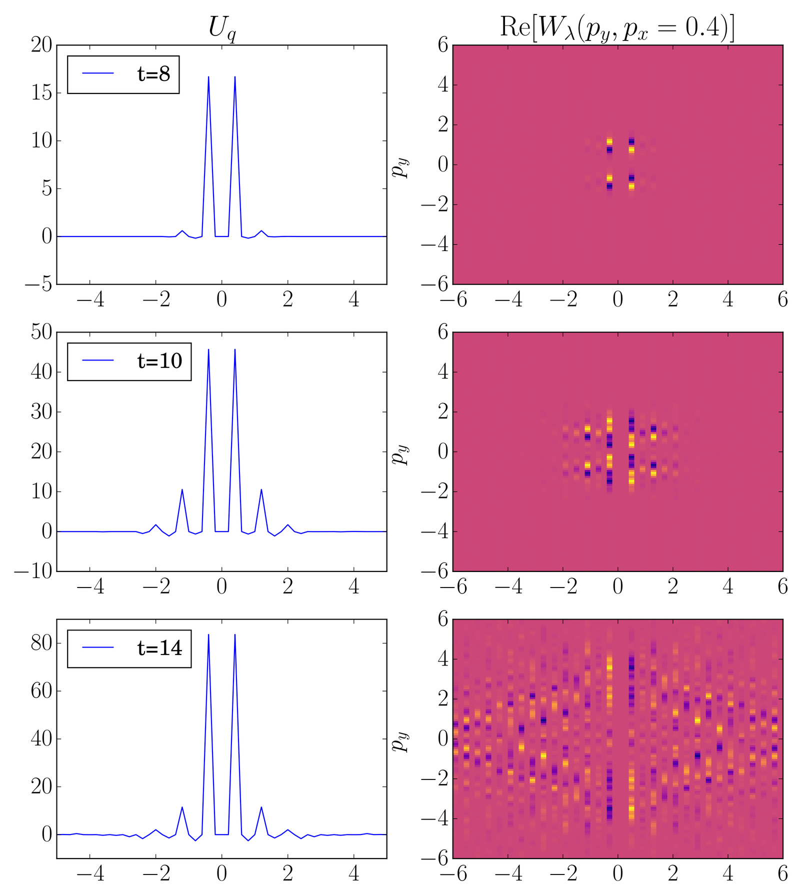

Figure 6: WM simulation of $q = 0.4 < 1$ in Fig. 3.

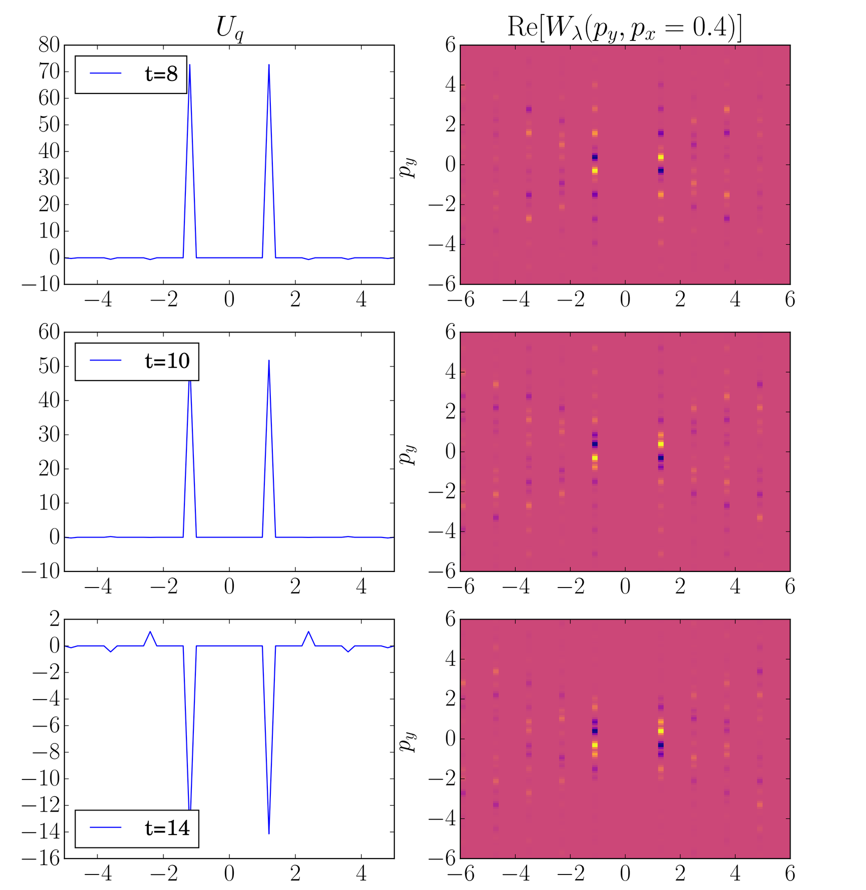

Figure 7: WM simulation of $q = 1.2 > 1$ in Fig. 3.

Conclusions

- The ZF wavenumber q plays an important role in ZF–DW interactions. Hence, the GO approximation $q^2 \ll 1$ is typically inadequate and the full-wave Wigner–Moyal modeling is needed.
- The TI growth rate is calculated. It is shown that the TI develops only if $q > 1$. Also, the ZI cannot be qualitatively predicted by the WKE if $q > 1$.
- The PP oscillations are found to be a genuine behavior if $q > 1$. The role of q can be qualitatively explained by analyzing the DW phase-space structure. A quantitative theory is yet to be developed.

References (a lot more to cite but no space!)

[1] H. Zhu, Y. Zhou, D. E. Ruiz, and I. Y. Dodin, arXiv:1712.08262.

[2] H.-L. Kuo, J. Meteor. **6**, 105 (1949).

[3] D. E. Ruiz, J. B. Parker, E. L. Shi, and I. Y. Dodin, Phys. Plasmas **23**, 122304 (2016).

[4] J. B. Parker, J. Plasma Phys. **82**, 595820602 (2016).

[5] E. L. Shi, G. W. Hammett, T. Stoltzfus-Dueck, and A. Hakim, J. Plasma Phys. **83**, 905830304 (2017).

[6] E.-J. Kim and P. H. Diamond, Phys. Rev. Lett **90**, 185006 (2003).